Journal of Cellular Biochemistry 95:268–280 (2005)

Fast Apoptosis and Erythroid Differentiation Induced by Imatinib Mesylate in JURL-MK1 Cells

Kateřina Kuželová,* Dana Grebeňová, Iuri Marinov, and Zbyněk Hrkal

Institute of Hematology and Blood Transfusion, U Nemocnice 1, 128 20 Prague 2, Czech Republic

Abstract We compare the effects of Imatinib mesylate (Glivec®) on chronic myeloid leukemia derived cell lines K562 and JURL-MK1. In both cell lines, the cell cycle arrests in G_1/G_0 phase within 24 h after the addition of 1 μM Imatinib. This is followed by a decrease of Ki-67 expression and the induction of apoptosis. In JURL-MK1 cells, the apoptosis is faster in comparison with K562 cells: the caspase-3 activity reaches the peak value (20 to 30 fold of the control) after about 40 h and the apoptosis proceeds to its culmination point, the DNA fragmentation, within 48 h following 1 μM Imatinib addition. Unlike K562 cells, JURL-MK1 cells possess a probably functional p53 protein inducible by TPA (tetradecanoyl phorbol acetate) or UV-B irradiation. However, no increase in p53 expression was observed in Imatinib-treated JURL-MK1 cells indicating that the difference in the apoptosis rate between the two cell lines is not due to the lack of p53 in K562 cells. Imatinib also triggers erythroid differentiation both in JURL-MK1 and K562 cells. Glycophorin A expression occurred simultaneously with the apoptosis, even at the single cell level. In K562 cells, but not in JURL-MK1 cells, the differentiation process involved increased hemoglobin synthesis. However, during spontaneous evolution of JURL-MK1 cells in culture, the effects produced by Imatinib progressively changed from the fast apoptosis to the more complete erythroid differentiation. We suggest that the apoptosis and the erythroid differentiation are parallel effects of Imatinib and their relative contributions, kinetics and completeness are related to the differentiation stage of the treated cells. J. Cell. Biochem. 95: 268–280, 2005.

Key words: Imatinib mesylate; STI571; leukemia; apoptosis; erythroid differentiation

Imatinib mesylate (Glivec®, STI571) is considered to be the most effective and a relatively safe drug, which has so far been used to treat the chronic phase of chronic myelogenous leukemia (CML). This low molecular weight compound acts as an inhibitor of Bcr-Abl protein kinase, which is the molecular cause of the disease in the majority of patients [Goldman and Melo, 2003]. CML develops when a single pluripotent hematopoietic cell acquires the chromosomal translocation designated t(9;22)(q34;q11) giving rise to a unique fusion gene, termed *bcr-abl*. The deregulated tyrosine kinase activity of the Bcr-Abl protein maintains in permanent activation several signal transduction pathways, namely the JAK/STAT, Ras/MEK/ERK, and PI3/Akt pathway [Calabretta and Perrotti, 2004; Steelman et al., 2004]. As a result, the cell escapes from the regulation mechanisms of cell cycle progression and apoptosis and gains a proliferative and survival advantage over the cells not bearing the aberrant chromosome.

The mechanism of Imatinib action is only partially elucidated. The drug binds to the ATP-binding site of Bcr-Abl thereby inhibiting its tyrosine kinase activity. As expected, the Bcr-Abl protein is rapidly dephosphorylated, becomes inactive and the constitutive activation of the above mentioned signaling cascades is interrupted. Subsequently, the cell cycle progression is arrested and the cell frequently undergoes apoptosis [Deininger et al., 1997; Gambacorti-Passerini et al., 1997; Fang et al., 2000; Horita et al., 2000; Pattacini et al., 2004].

K562 cell line, which is probably the most widely used experimental model of CML, was established in 1970 from a CML patient in blast crisis [Lozzio and Lozzio, 1975]. This cell line is

Abbreviations used: CML, chronic myelogenous leukemia; FITC, fluorescein isothiocyanate; Hb, hemoglobin; PE, phycoerythrin; PI, propidium iodide; TMB, tetramethylbenzidine; TPA, tetradecanoylphorbol 13-acetate.

Grant sponsor: Grant Agency of the Ministry of Health, Czech Republic; Grant number: NL 7681-3.

*Correspondence to: Kateřina Kuželová, Institute of Hematology and Blood Transfusion, U Nemocnice 1, 128 20 Prague 2, Czech Republic. E-mail: kuzel@uhkt.cz

Received 16 August 2004; Accepted 1 December 2004

DOI 10.1002/jcb.20407

unusual in that the t(9;22)(q34;q11) cytogenetic products usually associated with CML are absent. However, the abnormal CML-specific *bcr-abl* fusion gene is present and amplified by tandem repeats [Wu et al., 1995; Rodley et al., 1997; Drexler et al., 1999]. The resistance of these cells to apoptosis is further strengthened due to the lack of a functional p53 protein. In fact, one of p53 alleles is lost while the other one carries a frameshift mutation causing a premature translation stop [Law et al., 1993]. K562 cells have been used especially for studies of leukemic differentiation, but a large number of papers reporting on different effects of Imatinib mesylate on this cell line have emerged during the past few years. As for some other CML lines and patients' primary cells, Imatinib was shown to induce a cell cycle arrest in the G_1/G_0 phase, a decrease in the mitochondrial membrane potential, phosphatidylserine externalization, caspases activation and DNA fragmentation [Gambacorti-Passerini et al., 1997; Dan et al., 1998; Mow et al., 2002; Jacquel et al., 2003]. The effect of Imatinib on K562 cells is at least in part mediated by dephosphorylation of various proteins involved in signal transduction pathways, including ERK1/2 [Jacquel et al., 2003; Traina et al., 2003], STAT5 [Horita et al., 2000; Jacquel et al., 2003], and IRS1 [Traina et al., 2003]. The cytotoxic effect of Imatinib appears to be further increased by caspase-dependent cleavage of the inhibited Bcr-Abl protein [Jacquel et al., 2003]. Besides apoptosis, Imatinib mesylate was found to also trigger the erythroid differentiation of K562 cells as documented by an increase in the hemoglobin content [Fang et al., 2000], an upregulation of glycophorin A gene expression and positive benzidine staining of the treated cells [Jacquel et al., 2003; Kohmura et al., 2004]. A necrosis-like, caspase-independent cell death was observed in Imatinib-treated K562 and BV173 cells if the apoptosis was blocked by pan-caspase inhibitors [Okada et al., 2004].

The JURL-MK1 cell line was established in 1994 [Di Noto et al., 1997] and remains almost unexplored [only the work by Catani et al. 2001 was published to date]. To our knowledge, this is the first report about Imatinib treatment of this cell line. Unlike K562 cells, no defect of the gene encoding for p53 protein is known in JURL-MK1 cells. Megakaryocytic differentiation of JURL-MK1 cells can be obtained by the phorbol ester TPA while other inducers of differentiation (hemin, DMSO, Ara-C, ATRA) were reported to produce no effect [Di Noto et al., 1997].

In this study, we describe the kinetics of different processes induced by Imatinib mesylate in JURL-MK1 and K562 cells. We found that the apoptosis as well as the loss of Ki-67 expression is faster and more complete in JURL-MK1 cells. This difference is probably not due to the absence of a functional p53 in K562 cells as we detected no increase in p53 expression during the incubation of JURL-MK1 cells with Imatinib. We also show that erythroid differentiation occurs, at least partially, in both cell lines and that the apoptosis and the erythroid differentiation are not mutually exclusive at the single cell level. Finally, we suggest that the relative contribution of the two processes to overall Imatinib effect depend on the cell differentiation stage. The apoptosis becomes slower and the erythroid differentiation more complete during spontaneous cell progression along the erythroid differentiation pathway.

MATERIALS AND METHODS

Chemicals

Imatinib mesylate (formerly STI571, Glivec®) was kindly provided by Novartis (Basel, Switzerland). It was dissolved in distilled sterile water at 10 mM stock and stored at −20°C. Propidium iodide and fluorogenic substrate Ac-DEVD-AFC were purchased from Sigma (Prague, Czech Republic), FIX&PERM cell permeabilization kit from An Der Grub (Kaumberg, Austria), FITC-conjugated mouse anti-human Ki-67 antibody set from BD Biosciences (San Diego, CA). FITC-conjugated anti-glycophorin A and APO 2.7 Kit were obtained from Coulter/Immunotech (Prague, Czech Republic). The mouse anti-p53 monoclonal antibody from Stressgen (Victoria, BC, Canada) is known to detect 53 kDa protein on Western-blots with samples from humans, mice, rats, hamsters, and monkeys. The FITC-conjugated anti-p53 monoclonal antibody (Dako A/S, Denmark), which we used for flow-cytometry staining, recognizes an epitope in the N-terminus of the human p53 protein (both wild type and mutant type).

Cell Culture

K562 cells were purchased from the European Collection of Animal Cell Cultures (Salisbury,

UK), JURL-MK1 cells from DSMZ (German Collection of Microorganisms and Cell Cultures, Braunschweig, Germany). Cells were cultured in RPMI 1640 medium supplemented with 10% fetal calf serum, 100 U/ml penicillin, and 50 μg/ml streptomycin at 37°C in 5% CO_2 humidified atmosphere. They were diluted to a density of 2×10^5 cells per ml (2 to 4×10^5 for JURL-MK1 cells) three times a week. The observed doubling time was 20 to 30 h for both cell lines.

Cell Viability

Loss of cell viability after Imatinib treatment was assessed by flow cytometry of propidium iodide (PI) stained cells using a Coulter Epics XL flow cytometer as previously described [Grebeňová et al., 1998].

Cell Cycle Analysis

The cells (3×10^5) were collected by centrifugation, suspended in 4.5 ml of cold 70% ethanol, incubated for 30 min at 10°C and kept for 5 to 7 days at −20°C. The sample was then washed once in PBS and incubated for 30 min at room temperature in 1 ml of the modified Vindelovs propidium iodide buffer (10 mM Tris, pH 8, 1 mM NaCl, 0.1% Triton X-100, 20 μg/ml PI, and 10 K units ribonuclease A). The red fluorescence excited at 488 nm was then measured using Coulter Epics XL flow cytometer. The histograms of DNA content were analyzed using the G_1/G_2M Only Fit method.

Ki-67 Staining

Ki-67 expression in control and Imatinib-treated cells were assessed using a FITC-conjugated anti-human Ki-67 antibody. The cells (1×10^6) were washed, fixed, permeabilized, and labeled following the methanol modification of the staining protocol provided with the FIX&PERM permeabilization kit (modified protocol from Biozol Diagnostica Vertrieb GmbH, Germany). The fraction of Ki-67 expressing cells was determined by flow cytometry.

Caspase-3 Activity

Caspase-3 activity was determined by fluorometric measurement of the kinetics of 7-amino-4-trifluoromethyl coumarin (AFC) release from the fluorogenic substrate Ac-DEVD-AFC in the presence of cell lysates as previously described [Grebeňová et al., 2003].

DNA Fragmentation

The fraction of cells containing apoptotic DNA breaks was measured by TUNEL assay employing the In Situ Cell Death Detection Kit, Fluorescein (Roche Diagnostics GmbH, Mannheim, Germany) following the standard manufacturer's protocol. The extent of DNA labeling with fluorescein-dUTP was determined by flow cytometry.

p53 Expression

For Western-blot analysis of p53 expression, the cells (5×10^6) were suspended in a lysis buffer containing 0.15 M NaCl, 1 mM phenylmethylsulfonylfluoride (PMSF), and 0.5% Triton X-100 and kept for 30 min on ice. Western blots were prepared as previously described [Grebeňová et al., 2003], incubated with anti-p53 antibody, washed in TBS-T (Tris-buffered saline, 0.1% Tween 20) and incubated with the horseradish peroxidase-conjugated anti-mouse secondary antibody. The antigen was detected using the enhanced chemiluminescence Western blotting detection system ECL + PLUS (Amersham Pharmacia Biotech, UK) according to the manufacturer's instructions and visualized by autoradiography on X-ray film.

The expression level of p53 protein was also assessed using a FITC-conjugated monoclonal mouse anti-human p53 antibody. The cells (1×10^6) were fixed and permeabilized (FIX&PERM kit), labeled by the antibody and analyzed using Coulter Epics XL flow-cytometer.

Glycophorin A and 7A6 Expression

The cells (1×10^6) were harvested, washed in PBS, and fixed using reagent A of the FIX&PERM permeabilization kit according to the standard manufacturer's protocol. They were labeled by FITC-conjugated anti-glycophorin A antibody, washed and analyzed by flow cytometry. Alternatively, the fixed primary labeled cells were permeabilized employing reagent B of the FIX&PERM kit and further labeled by PE-APO 2.7, the antibody against the mitochondrial apoptotic marker 7A6. The red and green fluorescence signals from individual cells were then simultaneously analyzed by flow cytometry.

Hemoglobin Content

The increase in hemoglobin content was documented by changes which occurred in the

absorption spectra of cell lysates after 65 h incubation with Imatinib. Both control and Imatinib-treated cells (5×10^6 cells in each sample) were washed in PBS, lysed in 1 ml distilled water by repeated freezing and thawing (3 cycles) and homogenized using a 25G injection needle. The supernatant was isolated by 10 min centrifugation at 2,500*g* (at 4°C) and further centrifuged for 45 min at 15,000*g*. The absorption spectra were recorded from 300 to 600 nm employing a Phillips PU 8710 spectrophotometer (Cambridge, UK). The spectrum of control cells contained essentially a large background progressively decreasing from 300 to 600 nm. Only a slight irregularity around 414 nm indicated the presence of a small amount of hemoglobin. On the contrary, the absorption spectrum of the lysate obtained from Imatinib-treated cells exhibited well-shaped peaks characteristic of hemoglobin which were superimposed on the background. The intensity of the main peak centered at 414 nm was of 0.15 A (after the background subtraction). The overall protein concentration was measured using Bio-Rad Protein Assay (Bio-Rad, München, Germany).

Catalytic activity of hemoglobin in the oxidation of tetramethylbenzidine (TMB) substrate is the basis of the method allowing for sensitive and well reproducible determination of the relative amount of hemoglobin in the cell lysate (kit Plasma hemoglobin, Sigma, Prague, Czech Republic). The cell lysates were prepared as for caspase-3 activity measurements: 5×10^6 cells were washed in PBS and lysed in 50 μl lysis buffer (10 mM HEPES, pH 7.4, 2 mM EDTA, 0.1% CHAPS, 5 mM DTT, 10 μg/ml pepstatin, 10 μg/ml aprotinin, and 1 mM PMSF) by repeated freezing and thawing. The supernatant was isolated by 30 min centrifugation at 13,000*g* and diluted 25 fold in glacial acetic acid (90%) containing 5 mg/ml TMB. The sample was mixed quickly with 0.3% hydrogen peroxide (1:1) and increasing absorbance at 600 nm was continuously monitored for 10 min. The slope of the linear absorbance increase (in A/min) was used as the relative value of hemoglobin amount in the sample.

The proportionality coefficient between the relative values of hemoglobin content obtained from absorption spectra and from the kinetics of TMB oxidation was determined by the measurement of Imatinib-treated K562 cells (giving a high signal). The concentration of hemoglobin was calculated using the known molar absorption coefficient of hemoglobin, $\varepsilon_{\mu M}(414\ \text{nm}) = 0.128$ [Gibson and Carey, 1977].

RESULTS

Dosing Conditions

To determine the optimal drug dose, we tested the effect of different Imatinib concentrations on the cell proliferation rate and viability (Fig. 1). The results obtained by cell counting (Fig. 1A,C) and propidium iodide (PI) permeability measurements (Fig. 1B,D) show that 1 μM Imatinib concentration, which is frequently used in in vitro studies, is suitable for both JURL-MK1 and K562 cells. This concentration was used in all subsequent experiments.

Cell Cycle Analysis

The fractions of cells in individual cell cycle phases were assessed during the incubation with Imatinib. Representative histograms of controls and Imatinib-treated cells are shown in Figure 2. A marked decrease of the cell fraction with partly or fully replicated DNA ($S + G_2/M$ phases) occurs within the first 22 h after Imatinib addition (Fig. 2B,F). Later on, an increasing number of cells accumulates in the sub-G_1 region of the cell cycle histograms. The pattern of DNA content distribution is different in JURL-MK1 and K562 cells: a well-defined sub-G_1 peak near the original G_1 position is formed in JURL-MK1 cell line (Fig. 2C) while a smear of cells with very low DNA content is present in K562 cell cycle histograms (Fig. 2G). The evolution of the cell fractions in the phases involving DNA replication ($S + G_2/M$) and that in G_1/G_0 phase is represented in Figure 2D,H. The apoptotic cell fraction emerging in the sub-G_1 region is shown in Figure 5B.

Ki-67 Expression

For further characterization of the perturbation of cell proliferation, we studied the effect of Imatinib on the expression of the nuclear and nucleolar proliferation marker Ki-67 as can be seen in Figure 3. Ki-67 staining is completely lost from JURL-MK1 cells after 48 h incubation with Imatinib. A significant, but less pronounced decrease in Ki-67 expression also occurs in K562 cells treated with the drug. No change in Ki-67 staining was observed in the controls.

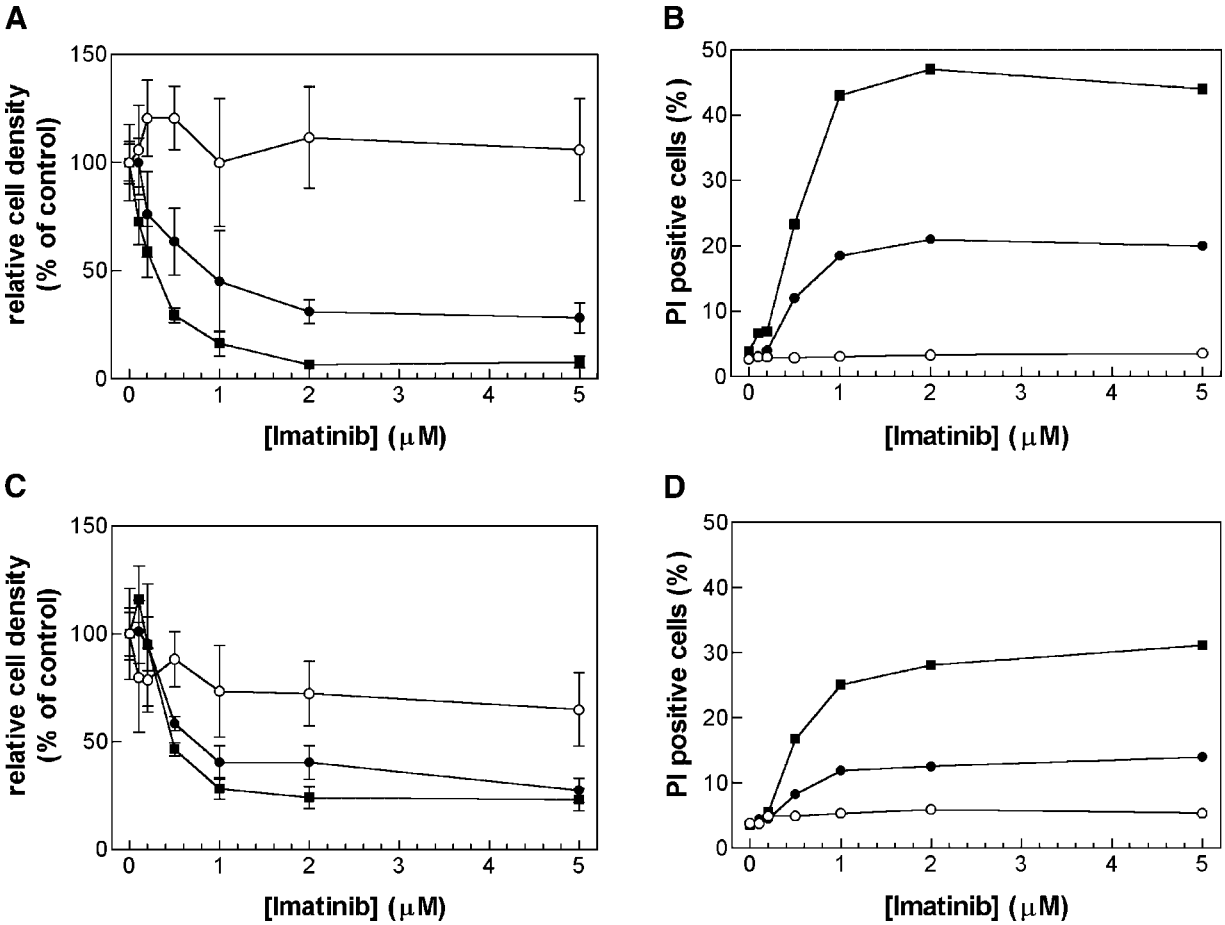

Fig. 1. Effect of Imatinib on the cell proliferation and cell death. **A**, **B**: JURL-MK1 cells, (**C**, **D**) K562 cells. Relative cell density (A, C) and propidium iodide positive cell fraction (B, D) were determined after 24 h (open circles), 48 h (closed circles), and 65 h (squares) of incubation with 0–5 μM Imatinib. The cell density of all samples was expressed as relative to the actual cell density of controls in the corresponding time points (100%). Results are representative from three experiments.

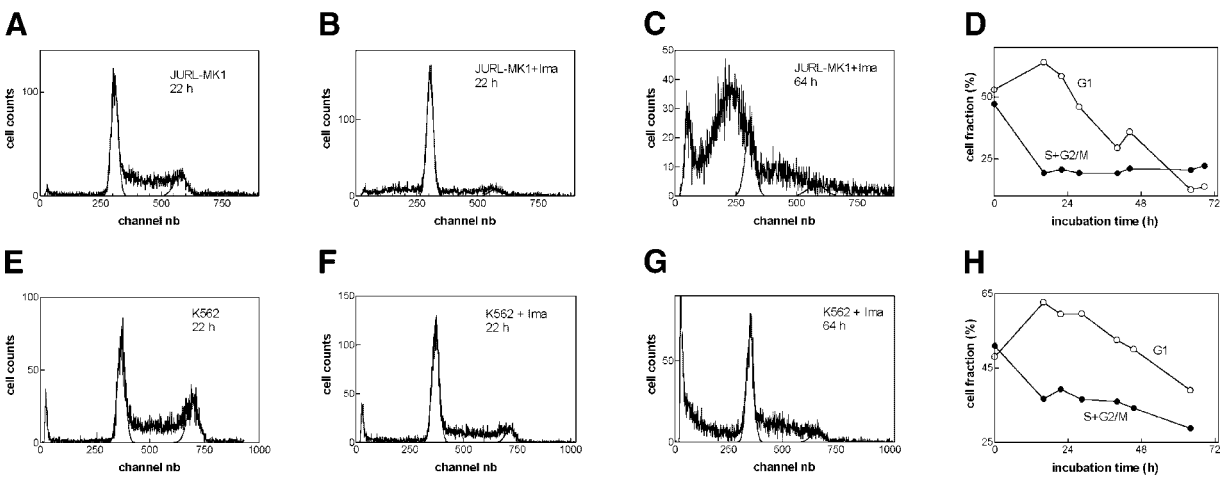

Fig. 2. Cell cycle analysis after Imatinib treatment. Representative histograms of JURL-MK1 cells (**A–C**) and K562 cells (**E–G**). A, E: Controls at 22 h; (B, F) cells after 22 h incubation with 1 μM Imatinib; (C, G) cells after 64 h incubation with 1 μM Imatinib. The evolution of the cell fraction in G_1/G_0 phases (open symbols) and $S + G_2/M$ phases (closed symbols) during Imatinib treatment is shown in panels (**D**) (JURL-MK1) and (**H**) (K562). The cell fraction in pre-G_1 phase is shown in Figure 5B.

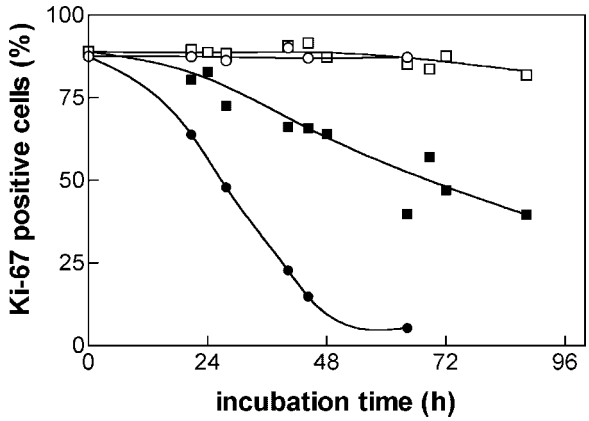

Fig. 3. Changes in Ki-67 expression during Imatinib treatment of JURL-MK1 (circles) and K562 cells (squares). Open symbols, controls; closed symbols, 1 μM Imatinib. Representative from three experiments.

Caspase-3 Activation

One of the most important apoptotic events, the caspase-3 activation, was monitored by the measurement of caspase-3 mediated cleavage of fluorogenic substrate. In JURL-MK1 cells, the caspase-3 activity reaches the maximal value (about 20 fold increase over the control) after about 40 h of incubation with Imatinib (Fig. 4). In K562 cells, the caspase-3 activation is more moderate and increases gradually for at least 64 h following the addition of Imatinib (about 6 fold increase over the control after 64 h).

DNA Fragmentation

DNA fragmentation is considered to be the hallmark of the culminating apoptotic process. The fraction of cells having reached this stage of the ordered autodestruction can be determined by the TUNEL method based on the enzymatic fluorescence labeling of DNA strand breaks. The results of the TUNEL analysis performed at different time intervals after Imatinib addition to JURL-MK1 and K562 cells are presented in Figure 5A. Again, we observed substantial difference in the apoptosis progression between the two cell lines. In JURL-MK1 cells, the DNA fragmentation is always achieved in 48 h after the addition of Imatinib. In contrast, K562 cells with fragmented DNA appear after more than 24 h incubation with Imatinib. The TUNEL positive cell fraction then progressively increases and it reaches 20%–50% within 64 h after the addition of Imatinib.

The fraction of cells undergoing DNA fragmentation can also be determined from the

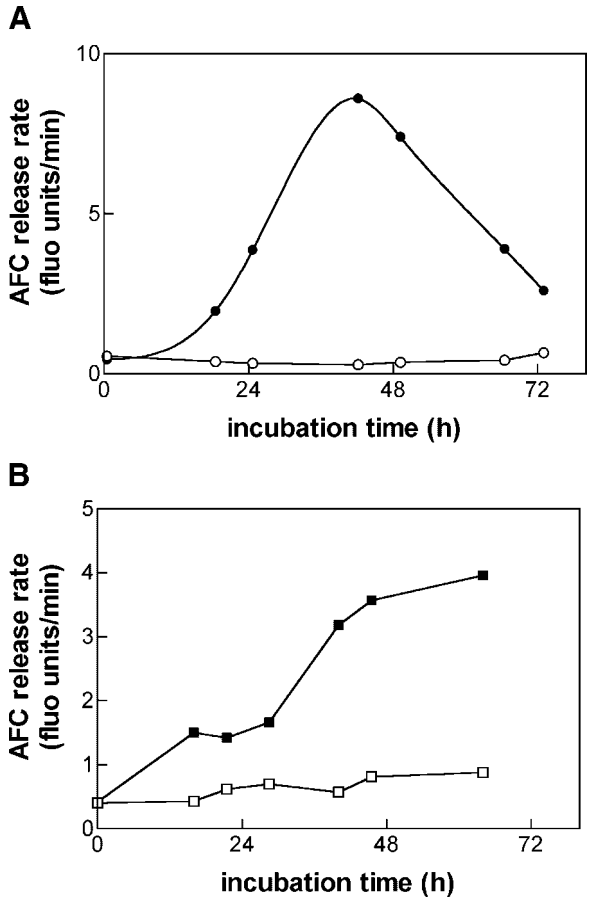

Fig. 4. Caspase-3 activation in JURL-MK1 (**A**) and K562 cells (**B**) during 1 μM Imatinib treatment. Representative of three independent experiments. Relative values of caspase-3 activity were determined from the rate of cleavage of fluorogenic substrate Ac-DEVD-AFC in presence of lysate obtained from control cells (open symbols) or Imatinib-treated cells (closed symbols).

histograms of DNA content (like those presented in Fig. 2C,G). The kinetic behavior of the sub-G_1 cell fraction (Fig. 5B) is in agreement with the data obtained by TUNEL method (Fig. 5A).

Plasma Membrane Permeabilization

The late stage of the apoptotic cell death is accompanied by a destabilization of the cell plasma membrane followed by the loss of cell integrity. Perturbation of the plasma membrane was assessed by the flow-cytometric measurement of PI uptake. In the controls, the fraction of PI stainable cells is always below 5% for both cell lines. The fraction of PI positive cells remains low during the first 40 h incubation with Imatinib. Later on, it starts to increase regularly (see e.g. closed circles and squares in Fig. 1B,D corresponding to PI positive cell

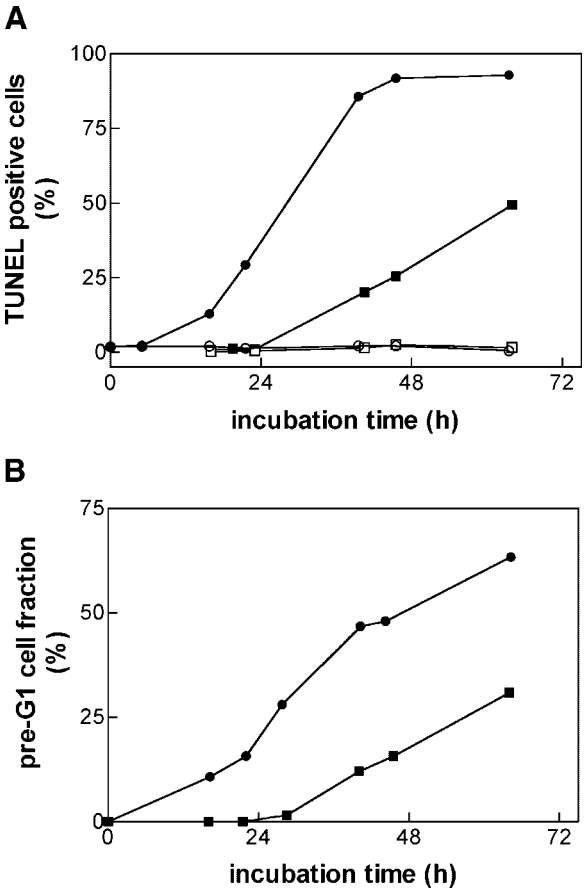

Fig. 5. Apoptotic DNA fragmentation induced by 1 μM Imatinib in JURL-MK1 (circles) and K562 cells (squares). **A**: Cell fraction with fragmented DNA as assessed using TUNEL method. Results are representative from three experiments. Open symbols, controls; closed symbols, Imatinib-treated cells. **B**: Cell fraction in pre-G_1 region of cell cycle histograms (examples shown in Fig. 2).

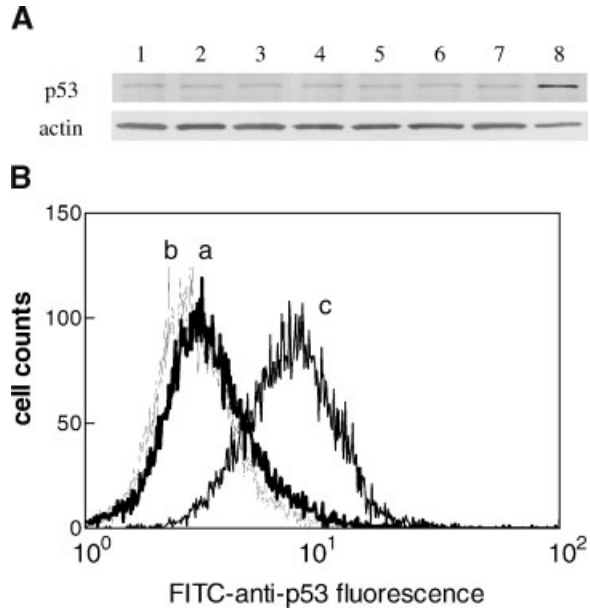

Fig. 6. p53 expression in JURL-MK1 cells during treatment with 1 μM Imatinib. Expression level of p53 protein was assessed by Western-blotting (**panel A**) and flow-cytometry (**panel B**). A: **Lanes 1–7**: Cells after 0, 3, 6, 10, 14, 18, and 24 h with Imatinib, (**lane 8**) cells treated by 10^{-7} M TPA for 65 h. B: Representative examples of traces obtained by flow-cytometric analysis following anti-p53 labeling. **a**: Control cells, (**b**) cells treated by Imatinib for 12 h, (**c**) cells irradiated with 1 J/cm^2 UV-B, 12 h after irradiation.

fractions at 48 and 65 h, respectively). In 65 h after 1 μM Imatinib has been added, the cell populations contains $46 \pm 5\%$ and $23 \pm 4\%$ of PI positive cells in JURL-MK1 and K562 line, respectively (means and s.d. from seven experiments).

p53 Expression

The expression level of p53 protein in JURL-MK1 cells was assessed both by Western-blotting and by flow cytometry employing a FITC-conjugated anti-p53 antibody. As illustrated in Figure 6A, no increase in p53 expression level was observed for up to 48 h of Imatinib treatment (tested every 3 to 4 h up to 24 h). This was confirmed by the flow-cytometry analysis (representative traces are shown in Fig. 6B). As a positive control of p53 expression, we included a sample of JURL-MK1 cells treated by 10^{-7} M TPA for 65 h (Fig. 6A: lane 8) or irradiated by 1 J/cm^2 dose of UV-B and subsequently incubated for 12 h at 37°C (Fig. 6B: trace c).

Erythroid Differentiation

Besides triggering apoptosis, Imatinib was also reported to induce erythroid differentiation in K562 cells [Fang et al., 2000; Jacquel et al., 2003; Kohmura et al., 2004]. We thus studied two processes characteristic of the erythroid differentiation: glycophorin A expression on the cell surface and hemoglobin synthesis. The results for both JURL-MK1 and K562 cell lines are represented in Figure 7. It follows that the fraction of cells exhibiting the erythroid surface marker glycophorin A markedly increases during Imatinib treatment in both JURL-MK1 and K562 cells (Fig. 7A).

The increase in hemoglobin content due to the Imatinib treatment was first documented by changes in the absorption spectra of the lysates obtained from K562 cells (see "Materials and Methods: Hemoglobin content"). Much more

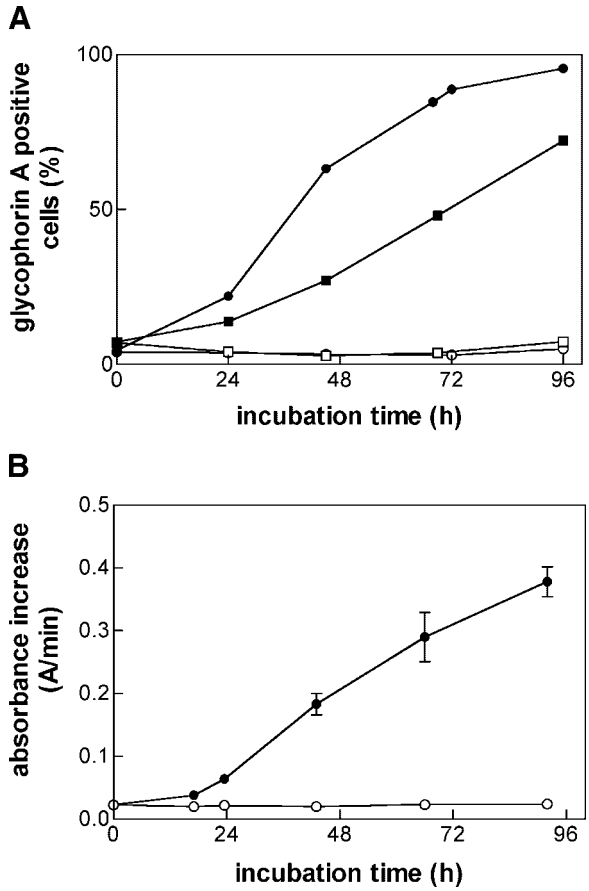

Fig. 7. Erythroid differentiation of JURL-MK1 and K562 cells induced by 1 μM Imatinib. **A**: Fraction of JURL-MK1 (circles) and K562 (squares) cells expressing glycophorin A. Control cells (open symbols) and cells with Imatinib (closed symbols) were labeled using FITC-conjugated anti-glycophorin A antibody and analyzed by flow-cytometry. Results are representative from three experiments. **B**: Relative hemoglobin content in the cell lysate obtained from control (open symbols) and Imatinib-treated (closed symbols) K562 cells as determined using TMB substrate oxidation. In JURL-MK1 cells, absorbance slope did not exceed 0.001 A/min both in control and Imatinib-treated cells. The points represent means and s.d. of three independent experiments.

sensitive determination of the relative hemoglobin content can be obtained by the method based on the catalytic activity of hemoglobin in the oxidation of TMB substrate. Using this method, we found that the basal hemoglobin level in JURL-MK1 cells is at least 20 fold lower than in K562 cells; the measured value (below 0.001 A/min) approaches the detection limit of the method. In the case of K562 cells, the hemoglobin content markedly increases during Imatinib treatment (Fig. 7B). In opposition to this finding, Imatinib failed to produce any change to the low basal hemoglobin level in JURL-MK1 cells.

TABLE I. Hemoglobin Content in K562 and JURL-MK1 Cells

	Hb molecules $\times 10^{-6}$/cell
JURL-MK1 basal level	≤ 0.4
K562 basal level	7–15
K562 + 65 h Imatinib	130–180

The relative value of hemoglobin content in the cell lysate was assessed using spectroscopic measurement of TMB substrate oxidation. The results were then expressed as an average number of hemoglobin copies in a single cell using the established correlation between the slope of the kinetic records and the hemoglobin absorption spectrum of Imatinib-treated cells. Given ranges correspond to limit values obtained from at least five independent experiments.

Using the relation coefficient between the relative values of hemoglobin content obtained from absorption spectra and from the kinetics of TMB oxidation and knowing the molar extinction coefficient of hemoglobin, we were able to estimate the average number of hemoglobin molecules in one single cell (Table I).

Correlation of Apoptosis and Erythroid Differentiation

Erythroid differentiation of K562 cells induced by Imatinib was suggested to be an alternative to the apoptosis [Jacquel et al., 2003]. However, regarding the large proportion of cells exhibiting both apoptotic and differentiation hallmarks, we concluded that these two pathways are likely to be activated simultaneously. To verify this hypothesis, we performed the parallel analysis of an apoptotic and a differentiation parameter in individual cells by means of flow-cytometry. We used a PE-labeled APO 2.7 antibody recognizing an early apoptotic marker (the mitochondrial antigen 7A6) simultaneously with the FITC-conjugated anti-glycophorin A antibody. Representative dotplots of JURL-MK1 and K562 cells, both control and incubated for 40 h with Imatinib, are shown in Figure 8. The control cells are both APO 2.7 and glycophorin A negative (LL quadrant). In JURL-MK1 cells, Imatinib treatment clearly triggers the simultaneous expression of both markers in a large number of cells (33%, UR quadrant). About a quarter of cells appears to only undergo the erythroid differentiation (LR quadrant). Only a small fraction of JURL-MK1 cells is slightly APO 2.7 positive without exhibiting glycophorin A staining (UL quadrant). After 65 h of Imatinib treatment, the prevailing fraction of cells (52%) was APO 2.7 and glycophorin A positive, while 21% and 6% of cells were in LR and UL quadrants (data not shown).

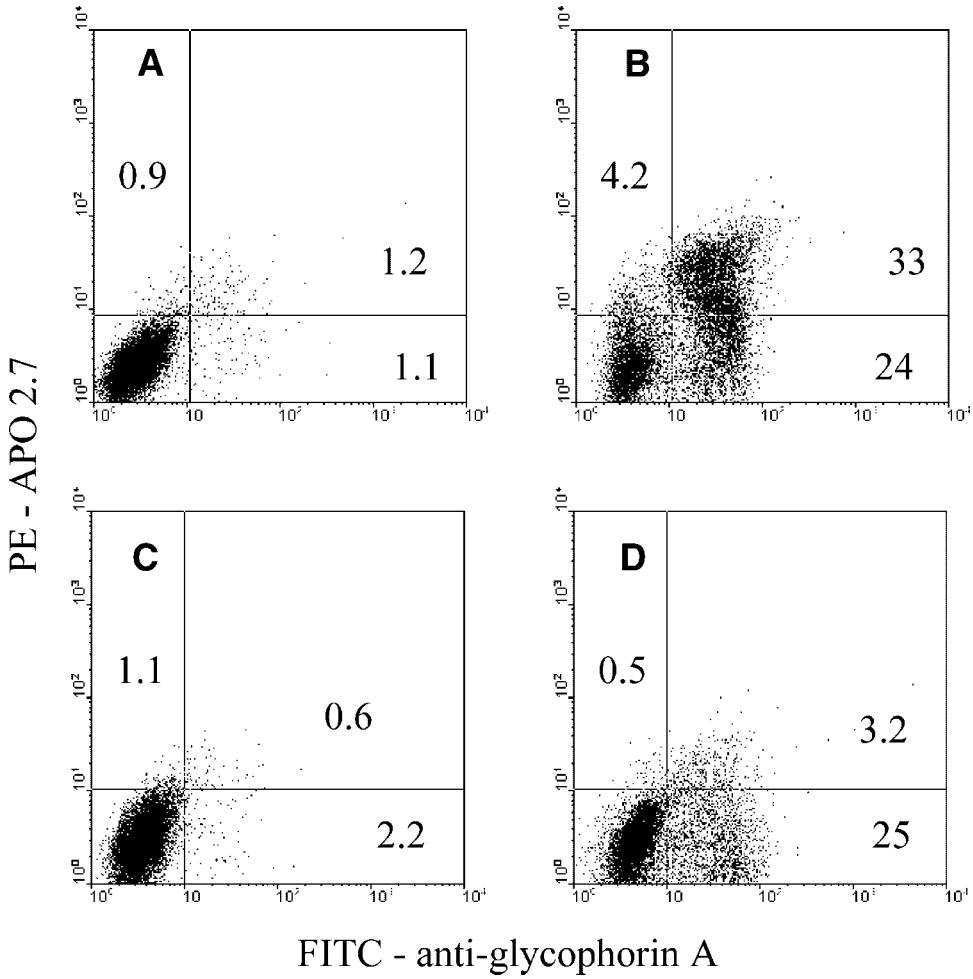

Fig. 8. Simultaneous induction of apoptosis and erythroid differentiation by 1 μM Imatinib. JURL-MK1 (**A**, **B**) and K562 (**C**, **D**) cells were labeled by FITC-conjugated anti-glycophorin A (x-axis) and PE-conjugated APO 2.7 (y-axis) antibodies and analyzed by flow-cytometry. A & C, Control cells; B & D, cells after 40 h incubation with Imatinib. Numbers indicate fraction of cells in the individual quadrants (in %). The experiment was repeated twice with similar results.

In the case of K562 cells, Imatinib firstly induces the glycophorin A expression (Fig. 8D, LR quadrant). However, this is later followed by the expression of APO 2.7 (13% cells in UR quadrant 65 h after Imatinib addition, data not shown). Similarly as for JURL-MK1 cells, the fraction of K562 cells undergoing apoptosis without glycophorin A expression is very low (about 2% after 65 h).

Spontaneous Evolution of JURL-MK1 Cells in Culture

We noted that some properties of JURL-MK1 cells were spontaneously modified after a prolonged cultivation in RPMI medium (described in "Materials and Methods"). The changes became apparent already after 5 months (about 70 passages) and striking differences have emerged from the comparison of freshly refrozen JURL-MK1 cells (about 10 passages) and an "aged" cell population (9 months in culture, split about 110 fold). The apoptotic process induced by Imatinib in "aged" cells was markedly delayed in comparison with the "fresh" cells. The kinetics and extent of changes detected in the individual apoptotic parameters (caspase-3 activation, expression of APO 2.7, DNA fragmentation—TUNEL) were very similar to those observed in K562 cells (see Figs. 4, 8, and 5). Furthermore, the basal level of hemoglobin in the "aged" cells determined using TMB substrate was at least 70 fold higher than the basal hemoglobin level in freshly refrozen JURL-MK1 cells, even exceeding that found in K562

cells. Consistently, Imatinib treatment of the "aged" JURL-MK1 population not only caused glycophorin A expression on the cell surface, but also enhanced hemoglobin synthesis. The relative hemoglobin content found in "aged" JURL-MK1 cells steadily increases during the Imatinib treatment and it reaches the value of about 0.3 A/min after 65 h. This corresponds to about 120 millions of hemoglobin molecules per cell (cf Fig. 7B and Table I for K562 cells). Thus, both apoptosis and erythroid differentiation induced by Imatinib proceed in a very similar way in "aged" JURL-MK1 and K562 cells.

We also noted that the spontaneous evolution of JURL-MK1 cell population is accompanied by a marked increase of the cell size which thus becomes comparable to that of K562 cells. In agreement with this finding, the protein content in the "aged" JURL-MK1 cells was more than 2 fold higher compared to the original cells (data not shown).

DISCUSSION

To date, little information is available about the JURL-MK1 cell line, which represents an interesting alternative to the widely used and well characterized line K562. The aim of this study was to investigate the processes induced both in JURL-MK1 and K562 cells by Imatinib mesylate, currently the leading compound in the treatment of CML in its chronic phase. We have compared the responses of the two cell lines to Imatinib and discuss possible reasons for the observed differences.

As in many other cell lines, Imatinib was found to stop the proliferation of both JURL-MK1 and K562 cells and to induce cell death. As is shown in Figure 1, these effects are dose-dependent and achieve a plateau phase for Imatinib concentration higher than 1 μM. This dose (1 μM Imatinib) was subsequently used in all experiments. The cell cycle analysis revealed that the cell cycle of Imatinib-treated cells arrests in the G_1/G_0 phase within the first 22 h of the treatment (Fig. 2B,F). The cell proliferation is tightly associated with the nuclear and nucleolar protein Ki-67. Although its function remains unclear, this protein was shown to be vital for cell proliferation [see Brown and Gatter, 2002, for a recent review]. Its complex and specific localization pattern within the nucleus changes during the cell cycle and its amount in the cell is highly regulated. In histopathology, the index of Ki-67 expression is commonly used in identifying tumors with malignant potential. To date, no data describing the effect of Imatinib mesylate on Ki-67 expression has been published to our knowledge. We found that Ki-67 staining is progressively lost from both JURL-MK1 and K562 cells during Imatinib treatment (Fig. 3). The decrease of the cell fraction expressing Ki-67 is faster and more complete in JURL-MK1 cells. The time frame and the extent of changes in Ki-67 staining appear to be tightly correlated with the increase of apoptotic cell fraction (cf Fig. 5). In comparison with K562 cells, the JURL-MK1 cell response to Imatinib treatment was also faster in all studied parameters related to apoptosis, i. e. caspase-3 activation (Fig. 4), expression of the apoptosis-related mitochondrial antigen 7A6 (Fig. 8) and DNA fragmentation (Fig. 5).

It has been shown that cooperation among Ras, STAT5 and PI3-K is required for full leukemogenic activities of Bcr-Abl [Sonoyama et al., 2002]. Among these signal pathways, Raf/MEK/ERK seems to be the most important. The ERK kinase cascade is a well recognized key regulator of mammalian cell proliferation promoting cell growth and inhibiting apoptosis. In addition, it is also involved in the regulation of differentiation processes [Woessmann and Mivechi, 2001]. In K562 cells, the constitutive activation of Raf/MEK/ERK by Bcr-Abl is rapidly disrupted by Imatinib treatment [Dan et al., 1998; Jacquel et al., 2003; Traina et al., 2003; Kohmura et al., 2004]. ERK1/2 dephosphorylation was shown to be dose-dependent; the maximal effect is achieved at 2 μM Imatinib [Traina et al., 2003]. JURL-MK1 cells carry only two copies of the *bcr-abl* gene, whereas more than 20 copies of bcr-abl were found in K562 cells [Wu et al., 1995; Rodley et al., 1997, and information obtained from the cell line provider]. Hypothetically, a higher amount of *Bcr-Abl* protein could account for a higher degree of activation of the above mentioned signaling pathways and it could explain lower efficiency of Imatinib in K562 cells. However, higher Imatinib concentration (up to 5 μM) only slightly accelerated the apoptosis in K562 cells: the maximal increase in the apoptotic cell fraction was about 20% of the value obtained for 1 μM Imatinib (data not shown, see Fig. 1 for the effect of Imatinib dose on the plasma membrane permeabilization). This indicates that the large

difference in apoptosis rate between JURL-MK1 and K562 cells cannot be explained by an incomplete inhibition of Bcr-Abl protein by 1 μM Imatinib in the latter cell line.

Another possible reason of this difference lies in the absence of the apoptosis activator p53 in K562 cells. The p53 tumor suppressor plays a critical role in the prevention of human cancer. In non-perturbed cells, the p53 protein is maintained at a low steady-state level through the action of Mdm2 protein, which promotes the ubiquitination and degradation of p53 by the proteasome. In response to various types of stress, p53 becomes stabilized and accumulates to a relatively high concentration. As a consequence, cells can undergo marked changes, ranging from increased DNA repair to apoptosis [Oren, 2003]. Previous studies have demonstrated a functional relationship between Bcr-Abl and p53. Effects of the constitutive tyrosine kinase activity of Bcr-Abl on protein expression were studied in systems containing inducible Bcr-Abl. Pierce et al. [2000] reported a decrease in p53 protein level after a prolonged exposure of FDCP-Mix cells to Bcr-Abl activity. In bcr-abl transformed BaF3 cells, Imatinib treatment resulted in a down-regulation of Mdm2 preceding the induction of apoptosis, which was partially p53-dependent [Goetz et al., 2001]. We therefore monitored the expression level of p53 protein during Imatinib treatment of JURL-MK1 cells by means of Western-blotting and flow-cytometry. Surprisingly, no detectable increase of p53 expression level occurred for up to 72 h of Imatinib treatment (representative examples are shown in Fig. 6A,B), although it was tested every 3 to 4 h up to 24 h. The response of JURL-MK1 cells to Imatinib is thus not mediated by an increase in p53 level and the difference in the apoptosis rate between JURL-MK1 and K562 cells can hardly be attributed to the presence or absence of this protein. In order to verify that p53 can be expressed in JURL-MK1 cells, we treated the cells also by TPA, which induces megakaryocytic differentiation [Di Noto et al., 1997], and by UV-B irradiation, which is known to induce p53 expression in many cell types. These positive controls (Fig. 6A: lane 8; Fig. 6B: trace c) confirm that p53 expression in JURL-MK1 cells probably occurs normally.

In the following part of this study, we focused on erythroid differentiation as a possible effect of Imatinib treatment, as it was presented in previously published reports [Fang et al., 2000; Jacquel et al., 2003; Kohmura et al., 2004]. The activation of p38 MAPK was recently shown to be crucial for Imatinib-induced erythroid differentiation, but not for the inhibition of proliferation in K562 cells [Kohmura et al., 2004]. Although the induction of erythroid differentiation in JURL-MK1 cells has not been described so far, our results show that JURL-MK1 is not only a megakaryocytic, but also an erythroid lineage. Actually, both JURL-MK1 and K562 cells exhibit marks of erythroid differentiation upon Imatinib treatment. Especially, the expression level of glycophorin A markedly increases in the majority of Imatinib-treated cells (Fig. 7A). It follows from the flow-cytometric analysis of double-labeled cells that erythroid differentiation and apoptosis are not mutually exclusive at the single cell level, as the early apoptotic marker 7A6 (detected by APO 2.7 antibody) and glycophorin A are simultaneously expressed in a large fraction of cells (Fig. 8). Another process characteristic of erythroid differentiation is the onset of hemoglobin synthesis. In K562 cells, the hemoglobin content increases in a similar way as the glycophorin A expression (Fig. 7B). The relative amount of hemoglobin measured employing TMB substrate oxidation was calibrated using the intensity of the absorption peak at 414 nm along with the known absorption coefficient of hemoglobin. We thus could calculate the average number of hemoglobin molecules in a single cell (Table I). In the case of Imatinib-treated cells, this number can be somewhat underestimated due to the lower total protein yield. In fact, the protein content in samples obtained from Imatinib-treated cells is about 2 fold lower in comparison with control cells. In any case, the number of hemoglobin molecules estimated to be present in a K562 cell after 65 h of Imatinib treatment is of the same order as the hemoglobin content in a mature erythrocyte (about 280 millions Hb molecules per cell). On the other hand, the results obtained for JURL-MK1 cells are quite different. The basal hemoglobin level of these cells is at least 20 fold lower in comparison with K562 cells and no increase of hemoglobin content was observed during Imatinib treatment. Thus, the erythroid differentiation induced by Imatinib in JURL-MK1 cells is incomplete, involving the glycophorin A expression, but not enhanced hemoglobin synthesis. We speculate that the rapidly processing

apoptosis in JURL-MK1 cells may not leave enough time to achieve erythroid maturation.

Surprisingly, the properties of JURL-MK1 cells change dramatically after several months of culture in RPMI 1640 medium. Besides an evident increase in the cell size, the progressive spontaneous evolution results in changes in the response to Imatinib treatment: the apoptosis is markedly delayed while the erythroid differentiation becomes more complete, also involving an increase of hemoglobin synthesis. With the exception of p53 expression after UV-B irradiation, the properties of these "aged" JURL-MK1 cells are very similar to that of K562 cells. As the basal hemoglobin level is also markedly elevated and even exceeds that found in K562 cells, we suggest that the observed evolution of JURL-MK1 cells corresponds to spontaneous progression along the erythroid differentiation pathway. In this case, the observed variability in the cell response to Imatinib treatment could be related to changes in the differentiation stage of the cell. Thus, it is possible that Imatinib induces fast apoptosis and partial erythroid differentiation in the early erythroid cells. On the other hand, the apoptosis can be reduced and the erythroid differentiation can become more complete when the cell is closer to the mature erythrocyte. This idea is supported by recent findings that inducers of differentiation prevent, at least partially, apoptosis and cell death caused by Imatinib in K562 cells. The simultaneous addition of phorbol esters inhibits Imatinib-mediated apoptosis and redirects differentiation of K562 cells towards the megakaryocytic program [Jacquel et al., 2003]. Erythropoietin, an endogenous factor required in erythroid differentiation, delays cell death induced by Imatinib and allows for establishing Imatinib-resistant clones of K562 cells [Kirschner and Baltensperger, 2003].

The overexpression of Bcr-Abl via genomic amplification was reported to be the predominant mechanism of resistance to Imatinib in in vitro models [Shah and Sawyers, 2003]. We cannot exclude the possibility that the observed spontaneous change of JURL-MK1 cells corresponds to a clonal evolution resulting in a multiplication of bcr-abl copies in a subpopulation of the "aged" JURL-MK1 cells. However, in this case, at least two separate cell populations should coexist in the culture and the kinetics of apoptotic changes would comprise several phases. As JURL-MK1 evolution involved an increase of the basal hemoglobin level, we think that the changes are more likely to be due to partial erythroid maturation.

In conclusion, the addition of Imatinib mesylate to JURL-MK1 cells results in simultaneous triggering of the apoptosis and the partial erythroid differentiation. The apoptosis proceeds markedly faster in comparison with K562 cells. This difference seems to be neither due to different number of *bcr-abl* gene copies nor to the lack of p53 protein in K562 cells. On the other hand, erythroid differentiation induced by Imatinib in JURL-MK1 cells is incomplete, as the increase of glycophorin A expression is not accompanied by a detectable increase of hemoglobin content. However, the spontaneous evolution of JURL-MK1 cells leads to a modification of cell response to Imatinib: the apoptosis is delayed, whereas erythroid differentiation becomes more complete including the onset of hemoglobin synthesis. We suggest that the apoptosis and the erythroid differentiation are parallel effects of Imatinib on proerythroid cells and that the relative contributions, kinetics and completeness of these processes are related to the differentiation stage of the treated cells.

ACKNOWLEDGMENTS

The authors thank Mrs. H. Pilcová and J. Sedlmaierová for the expert technical assistance.

REFERENCES

Brown DC, Gatter KC. 2002. Ki67 protein: The immaculate deception? Histopathology 40:2–11.

Calabretta B, Perrotti D. 2004. The biology of CML blast crisis. Blood 103:4010–4022.

Catani L, Amabile M, Luatti S, Valdre L, Vianelli N, Martinelli G, Tura S. 2001. Interleukin-4 downregulates nuclear factor-erythroid 2 (NF-E2) expression in primary megacaryocytes and in megacaryoblastic cell lines. Stem Cells 19:339–347.

Dan S, Naito M, Tsuruo T. 1998. Selective induction of apoptosis in Philadelphia chromosome-positive chronic myelogenous leukemia cells by an inhibitor of BCR-ABL tyrosine kinase, CGP57148. Cell Death Differ 5:710–715.

Deininger MWN, Goldman JM, Lydon N, Melo JV. 1997. The tyrosine kinase inhibitor CGP57148B selectively inhibits the growth of BCR-ABL-positive cells. Blood 90: 3691–3698.

Di Noto R, Luciano L, Lo Pardo C, Ferrara F, Frigeri F, Mercuro O, Lombardi ML, Pane F, Vacca C, Manzo C, Salvatore F, Rotoli B, Del Vecchio L. 1997. JURL-MK1 (c-kithigh/CD30-/CD40-) and JURL-MK2 (c-kitlow/CD30+/CD40+) cell lines: 'Two-sided' model for investi-

gating leukemic megakaryocytopoiesis. Leukemia 11: 1554–1564.

Drexler HG, MacLeod RA, Uphoff CC. 1999. Leukemia cell lines: In vitro models for the study of Philadelphia chromosome-positive leukemia. Leuk Res 23:207–215.

Fang G, Kim CN, Perkins CL, Ramadevi N, Winton E, Wittmann S, Bhalla KN. 2000. CGP57148B (STI-571) induces differentiation and apoptosis and sensitizes Bcr-Abl-positive human leukemia cells to apoptosis due to antileukemic drugs. Blood 96:2246–2253.

Gambacorti-Passerini C, Le Coutre P, Mologni L, Fanelli M, Bertazzoli C, Marchesi E, Di Nicola M, Biondi A, Corneo GM, Belotti D, Pogliani E, Lydon NB. 1997. Inhibition of the ABL kinase activity blocks the proliferation of BCR/ABL+ leukemic cells and induces apoptosis. Blood Cells Mol Dis 23:380–394.

Gibson QH, Carey FG. 1977. Effect of hydrostatic pressure on spectra of heme compounds. J Biol Chem 252:4098–4101.

Goetz AW, van der Kuip H, Maya R, Oren M, Aulitzky WA. 2001. Requirement for Mdm2 in the survival effects of Bcr-Abl and interleukin 3 in hematopoietic cells. Cancer Res 61:7635–7641.

Goldman JM, Melo JV. 2003. Chronic myeloid leukemia—Advances in biology and new approaches to treatment. N Eng J Med 349:1451–1464.

Grebeňová D, Cajthamlová H, Bartošová J, Marinov J, Klamová H, Fuchs O, Hrkal Z. 1998. Selective destruction of leukaemic cells by photoactivation of 5-aminolaevulinic acid-induced protoporphyrin IX. J Photochem Photobiol B: Biol 47:74–81.

Grebeňová D, Kuželová K, Smetana K, Pluskalová M, Cajthamlová H, Marinov I, Fuchs O, Souček J, Jarolím P. 2003. Mitochondrial and endoplasmic reticulum stress-induced apoptotic pathway are activated by 5-aminolevulinic acid-based photodynamic therapy in HL60 leukemia cells. J Photochem Photobiol B Biol 69:71–85.

Horita M, Andreu EJ, Benito A, Arbona C, Sanz C, Benet I, Prosper F, Fernandez-Luna JL. 2000. Blockade of the Bcr-Abl kinase activity induces apoptosis of chronic myelogenous leukemia cells by suppressing signal transducer and activator of transcription 5-dependent expression of Bcl-xL. J Exp Med 191:977–984.

Jacquel A, Herrant M, Legros L, Belhacene N, Luciano F, Pages G, Hofman P, Auberger P. 2003. Imatinib induces mitochondria-dependent apoptosis of the Bcr-Abl positive K562 cell line and its differentiation towards the erythroid lineage. FASEB J 17:2160–2162.

Kirschner KM, Baltensperger K. 2003. Erythropoietin promotes resistance against the Abl tyrosine kinase inhibitor imatinib (STI571) in K562 human leukemia cells. Mol Canc Res 1:970–980.

Kohmura K, Miyakawa Y, Kawai Y, Ikeda Y, Kizaki M. 2004. Different roles of p38 MAPK and ERK in STI571-induced multi-lineage differentiation of K562 cells. J Cell Physiol 198:370–376.

Law JC, Ritke MK, Yalowich JC, Leder GH, Ferrell RE. 1993. Mutational inactivation of the *p53* gene in the human erythroid leukemic K562 cell line. Leuk Res 17: 1045–1050.

Lozzio CB, Lozzio BB. 1975. Human chronic myelogenous leukemia cell-line with positive Philadelphia chromosome. Blood 45:321–334.

Mow BMF, Chandra J, Svingen PA, Hallgren CG, Weisberg E, Kottke TJ, Narayanan VL, Litzow MR, Griffin JD, Sausville EA, Tefferi A, Kaufmann SH. 2002. Effects of the Bcr/abl kinase inhibitors STI571 and adaphostin (NSC 680410) on chronic myelogenous leukemia cells in vitro. Blood 99:664–671.

Okada M, Adachi S, Imai T, Watanabe K, Toyokuni S, Ueno M, Zervos AS, Kroemer G, Nakahata T. 2004. A novel mechanism for imatinib mesylate-induced cell death of BCR-ABL-positive human leukemic cells: Caspase-independent, necrosis-like programmed cell death mediated by serine protease activity. Blood 103:2299–2307.

Oren M. 2003. Decision making by p53: Life, death and cancer. Cell Death Differ 10:431–442.

Pattacini L, Mancini M, Mazzacuratti L, Brusa G, Benvenuti M, Martinelli G, Baccarani M, Santucci MA. 2004. Endoplasmic reticulum stress initiates apoptotic death induced by STI571 inhibition of p210 bcr-abl tyrosine kinase. Leuk Res 28:191–202.

Pierce A, Spooncer E, Wooley S, Dive C, Francis JM, Miyan J, Owen-Lynch PJ, Dexter TM, Whetton AD. 2000. Bcr-Abl protein tyrosin kinase activity induces a loss of p53 protein that mediates a delay in myeloid differentiation. Oncogene 19:5487–5497.

Rodley P, McDonald M, Price B, Fright R, Morris C. 1997. Comparative genomic hybridization reveals previously undescribed amplifications and deletions in the chronic myeloid leukemia-derived K-562 cell line. Genes Chromosomes Cancer 19:36–42.

Shah NP, Sawyers CL. 2003. Mechanisms of resistance to STI571 in Philadelphia chromosome-associated leukemias. Oncogene 22:7389–7395.

Sonoyama J, Matsumura I, Ezoe S, Satoh Y, Zhang X, Kataoka Y, Takai E, Mizuki M, Machii T, Wakao H, Kanakura Y. 2002. Functional cooperation among Ras, STAT5, and phosphatidylinositol 3-kinase is required for full oncogenic activities of BCR/ABL in K562 cells. J Biol Chem 277:8076–8082.

Steelman LS, Pohner SC, Shelton JG, Franklin RA, Bertrand FE, McCubrey JA. 2004. JAK/STAT, RaF/MEK/ERK, PI3K/Akt and BCR-ABL in cell cycle progression and leukemogenesis. Leukemia 18:189–218.

Traina F, Carvalheira JBC, Saad MJA, Costa FF, Saad STO. 2003. BCR-ABL binds to IRS-1 and IRS-1 phosphorylation is inhibited by imatinib in K562 cells. FEBS Lett 535:17–22.

Woessmann W, Mivechi NF. 2001. Role of ERK activation in growth and erythroid differentiation of K562 cells. Exp Cell Res 264:193–200.

Wu S-Q, Voelkerding KV, Sabatini L, Chen X-R, Huang J, Meisner LF. 1995. Extensive amplification of *bcr/abl* fusion genes clustered on three marker chromosomes in human leukemic cell line K-562. Leukemia 9:858–862.